Seismic response of landslide with micropiles

Nan Li, Yuming Men, Ou Gao, Xueling Liu

School of Geology Engineering and Geomatics, Chang'an University, Xi'an, Shaanxi 710054, China

E-mail: linan1990111@163.com

Abstract: In order to study seismic response of the landslide with micropiles, shaking table tests were performed on two landslide models (i.e., micropiles-reinforced landslide and unreinforced landslide). El Centro waves, Wenchuan waves, Kobe waves and sinusoidal waves were applied to the model. A comparison was made on the acceleration response between reinforced landslide and unreinforced landslide. Furthermore, the residual bending moment of micropile was analyzed. The results indicate that micropiles have a good seismic performance for landslide, and it can suppress the seismic waves that propagated to landslide. Under the same seismic wave, the acceleration response of reinforced landslide is smaller than that of unreinforced, especially in the toe of landslide. The residual bending moment of micropiles shows reverse "S"-type. The maximum residual bending moment of micropile mainly distribute in 3.7 times pile diameter above the sliding surface and 1.4 times pile diameter below the sliding surface.

1. Introduction

China is the area with high occurrence rate of earthquake. If the earthquake happens, massive geological hazards will occur. Landslide induced by earthquake is one of the major seismic geological hazards. For example, the earthquake with a magnitude of 8.0 (MS) struck Wenchuan, Sichuan Province, China on May 12, 2008. There were about 56,000 rockfalls and landslides triggered directly in Wenchuan Earthquake, forming 256 barrier lakes [1,2]. Ensuring the safety of seismic areas and studying the earthquake-resistant mechanism of various support structures have become an urgent demand for social and economic development in China.

Micropile is one of the new support structures, which is generally defined as small-diameter (typically less than 300 mm), drilled and grouted replacement piles that are typically reinforced[3]. Compared to traditional antisliding piles, micropile group is relatively simple, fast, environmental-friendly and economic. In addition, micropiles can be readily installed in areas with limited equipment access, such as for landslides located in hilly, steep, or mountainous areas[4].

Recently, with the rapid development of micropiles in slope or landslide, mechanical characteristics, damage modes and the optimal pile space were studied by many scholars[4-6]. However, most researches are mainly about the stress of piles under static loadings, and only limited studies are available on the dynamic behavior of micropiles in landslide under earthquake. So based on large-scale shaking table model test, the model landslide supported by micropiles was conducted, and acceleration responses of landslide, and mechanical characteristics of micropile were analyzed respectively in this paper.

2. Shaking table model test

The model landslide tests were performed on large-scale shaking table established at the Key Laboratory of Structure and Earthquake Resistance in Civil Engineering, Xi'an University of Architecture and Technology. The size of the table was 4.1 m × 4.1 m, and the capacity of the table was 20 t. The maximum acceleration was ±1.5, ±1.0, and ±1.0 g in the X, Y and Z directions, respectively. The frequency of the input motion ranged from 0.1 to 50 Hz.

The model landslide was installed into a rigid model box with a length of 2.6 m, width of 1.4m, and height of 1.6 m. Tempered glass was used as the left and right sides of the model box to observe the deformation of the soil mass. Before the construction of the model, small cobblestones (the maximum particle-size is 2.5) were pasted at the bottom of the box to reduce the relative displacement between the soil and the box. In order to reduce the energy reflection of the model box to the incident wave, 10-cm-thick cystosepiment was pasted on both the front and back of the box.

2.1. Test prototype and law of similitude

The shaking table test model was designed based on a homogeneous soil landslide. The landslide height is 12.8 m. The sliding mass has three parts: 2# slope (slope ratio: 1:0.59), platform (3.04 m wide) and 1# slope (slope ratio: 1: 0.75). Reinforced concrete micropiles were vertically driven into the platform. The micropiles were divided into three rows, and the pile bolcks of micropiles were connected with concrete plate. The pile length, pile diameter, pile spacing and row spacing were 8.4 m, 28 cm, 1.96 m（7 times pile diameter）and 1.12 m（4 times pile diameter）respectively.

According to theorem of Bockingham π [7], geometric similarity, physical similarity and mechanical similarity should be considered in this study. Based on the size and bearing capacity of the shaking table, size of the soil container, boundary effect and some other factors, the length scale factor is set to be 8:1 (prototype: model). The similitude ratios of the model structure and soil are listed in Table 1.

In order to study the dynamic response of the landslide before and after reinforced with micropiles, two model landslides were performed: micropiles-reinforced landslide and unreinforced landslide. The model profiles are shown as Figure 1.

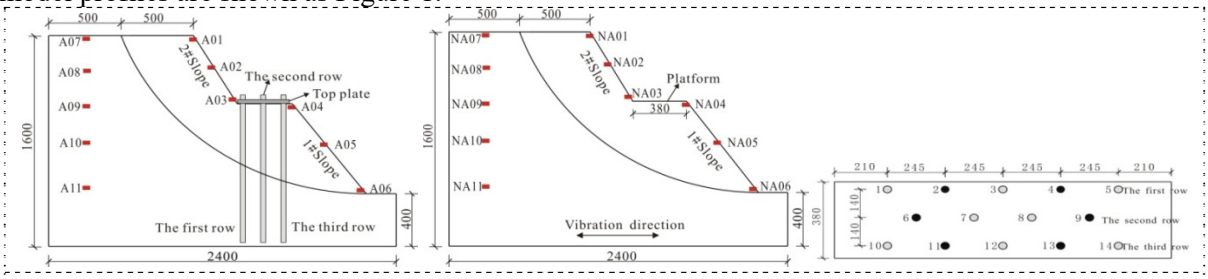

（a）Reinforced landslide （b）Unreinforced landslide (c) Layout of micropiles in platform

Figure 1. The model profiles（unit：mm）

Table 1. Law of similitude of the prototype landslide and model landslide

Parameters	Similarity law	Similarity constants	Remarks
Geometry (L)	C_L	8	Control variable
Elasticity modulus (E)	C_E	3	Control variable
Flexural stiffness (EI)	$C_{EI}= C_E C_L^4$	12288	
Stress (σ)	$C_\sigma= C_E$	3	
Strain (ε)	C_ε	1	
Poisson ratio (μ)	C_μ	1	
Density(ρ)	C_ρ	0.75	Control variable
Mass (m)	$C_m=C_\rho C_L^3$	384	

Stiffness (K)	$C_K=C_EC_L$	24
Time (t)	$C_t=(C_m/C_k)^{1/2}$	4
Frequency (f)	$C_f=1/C_t$	0.25
Acceleration (a)	$C_a=C_L/C_t^2$	0.5

2.2. Similar materials and setup of the model

2.2.1. Sliding bed and sliding mass.

The sliding bed and sliding mass were homogeneous soil, which was mainly formed by clay, barite powder, quartz and bentonite powder at ratios of 0.5：0.3：0.06：0.14. The model of sliding bed and sliding mass were constructed by filling soil to the model box layer upon layer. Direct shear tests were performed on the soil specimens obtained from the model landslide. The shearing strength parameters of materials are shown in Table 2.

The sliding surface was designed to be a circular arc, which was determined by the limit equilibrium method. Sliding soil was simulated by placing duplex plastic paper on the sliding bed. The cohesive force and internal friction angle of the sliding band were 3.5 kPa and 16°, respectively.

Table 2. Results of the direct shear tests on soil specimens

Position	Water content	Unit weight	Cohesion	Compression modulus	Internal friction angle
Sliding mass	13.9%	2.03 kN/m^3	11.82 kPa	6.57 Mpa	26°
Sliding bed	15.0%	2.11 kN/m^3	12.32 kPa	7.24 Mpa	28°

2.2.2. Model micropile and top plate in micropiles.

The micropile model was precast pile that prepared before the shaking test, and longitudinal steel in micropile is aluminum material (reinforcement form: 4Φ6). The casting material of micropile model was plaster (the water-gypsum ratio was 0.7, and the compressive strength was 11.1 Mpa). After 18 days of natural maintenance, marine glue was evenly smeared on the surface of micropile to improve the waterproofing quality. In order to simulate the interaction between pile and soil, quartz sands were pasted on the surface of micropiles.

The modelling process：fixing model piles to preset position→ making sliding bed by ramming soil layer upon layer→ making sliding surface by cutting sliding bed based on sliding surface shape→ placing duplex plastic paper on the sliding bed→ making sliding mass→ installing top plate to each pile bolck→ fixing landslide models to the shaking table. The final landslide model is shown in Figure 2.

Figure 2. Test model landslide

2.3. Measuring scheme

In order to monitor the acceleration response of landslides, six accelerometers were installed on the landslide surface (reinforced landslide: A01-A06; unreinforced landslide: NA01-NA06 shown in Figure1). Five accelerometers were embedded in landslide body along the vertical direction (reinforced landslide: A07-A11; unreinforced landslide: NA07-NA11). In order to compare the

acceleration response of the two landslides, layout of accelerometers of unreinforced landslide was nearly the same to reinforced landslide.

Two piles were selected as test piles in each row. Piles 2 and 4 were selected for the first row of piles, piles 6 and pile 9 were selected for the second row of piles, and piles 11 and 13 were selected for the third row of piles (shown in Figure 1c). Eight strain gauge couples were glued to the pile to measure bending strains of micropile, as shown in Figure 3.

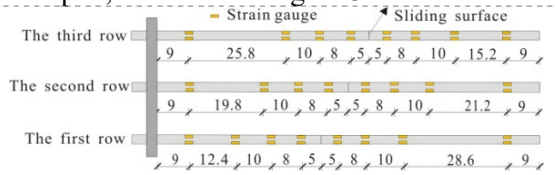

Figure 3. Layout of strain gauges（unit: cm）

2.4. Loading schemes

There were four different seismic waves applied to the test: El Centro waves, Wenchuan waves , Kobe waves and sinusoidal waves (4 Hz, 8 Hz, 12 Hz). Because horizontal earthquakes are the major cause of structure destruction and can significantly reduce the slope stability, all waves are loaded in the horizontal direction in the test.

In order to get the natural frequency, damping ratio and other dynamic parameters of the anchorage landslide model, white noise waves were input when the acceleration loading amplitude was changed. The loading schemes in the test are listed in Table 3.

Table 3. Loading schemes

Number	Input waves	Amplitude	Number	Input waves	Amplitude
1	W-1	0.03 g	19	W-4	0.03
2, 3, 4	Wen-1, Wen-1, Ko-1	0.1 g	20, 21, 22	Wen-4, Wen-4, Ko-4	0.4
5, 6, 7	4Hz-1, 8 Hz-1, 12Hz-1	0.1 g	23	W-5	0.03
8	W-2	0.03 g	24, 25, 26	Wen-5, Wen-5, Ko-5	0.4
9, 10, 11	Wen-2, Wen-2, Ko-2	0.2	27	W-6	0.03
12, 13, 14	4Hz-2, 8 Hz-2, 12Hz-2	0.2	28, 29, 30	Wen-6, Wen-6, Ko-6	0.6
15	W-3	0.03	31	W-7	0.03
16, 17, 18	Wen-3, Wen-3, Ko-3	0.3	—	—	—

3. Results and Analysis

3.1 Test phenomenon

After each excitation, cracks of landside were observed, measured and recorded. Figure 4 shows the details of test phenomenon.

(1) Micropiles-reinforced landslide

After 0.1~0.2 g, the reinforced landslide had no significant phenomenon. After 0.3 g, a 4 cm long tension crack A-B was generated between the second row of piles and the third row of piles (shown in Figure 4a). After 0.4 g El Centro waves, crack A-B extends to C, and the crack width was about 0.8 cm. Meanwhile, the pile-up landslide began to slide. The landslide toe moved by 0.6 cm and the crest was 0.4 cm. After 0.4 g Wenchuan waves, crack A-B-C continued to widen and extended downwards to point D. The cumulative displacement of the toe was 3 cm and cumulative settlement at the crest was 2.3 cm. After 0.4 g Kobe waves, tensile cracks F-G (5 cm long) reappeared front of the first row of piles, and cracks A-B-C-D extended to point E. After 0.6 g El Centro waves, the sliding mass continued to slide and the crack continued to expand. After 0.8 g Kobe waves, the cumulative horizontal displacement of the toe was 4.1 cm, and the settlement of crest was 3.4 cm.

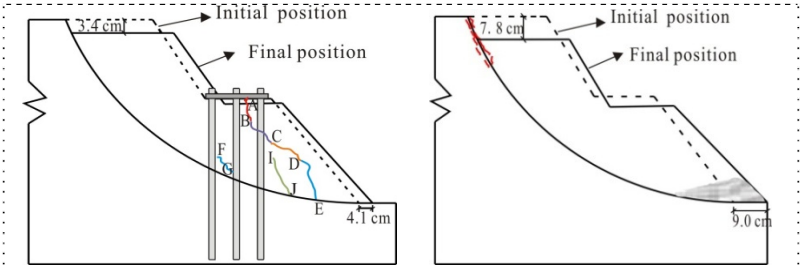

（a）Reinforced landslide （b）Unreinforced landslide

Figure 4. Deformation modes of model landslides and the development of cracks

(2) Unreinforced landslide

After 0.1 g, unreinforced landslide had no significant phenomenon. After 0.2 g Kobe waves, there were some hairline cracks near slide surface on the top part, and these hairline cracks had the same direction with sliding surface (seen in Figure 4b). After 0.2 g 12 Hz sinusoidal waves, the sliding mass slided quickly along the sliding surface with a horizontal displacement of 8.0 cm. After 0.3 g Wenchuan waves, the toe moves 9.0 cm horizontally and the settlement of crest was 7.8 cm. At the same time, the soil at the toe became looser than before, and the entire sliding mass accumulated on the front side of the box.

3.2 The comparison of acceleration response

Figure 5 shows several acceleration histories of A01, NA01, A04, NA04, A05, NA05, A06, NA06 under 0.1 g El Centro waves.

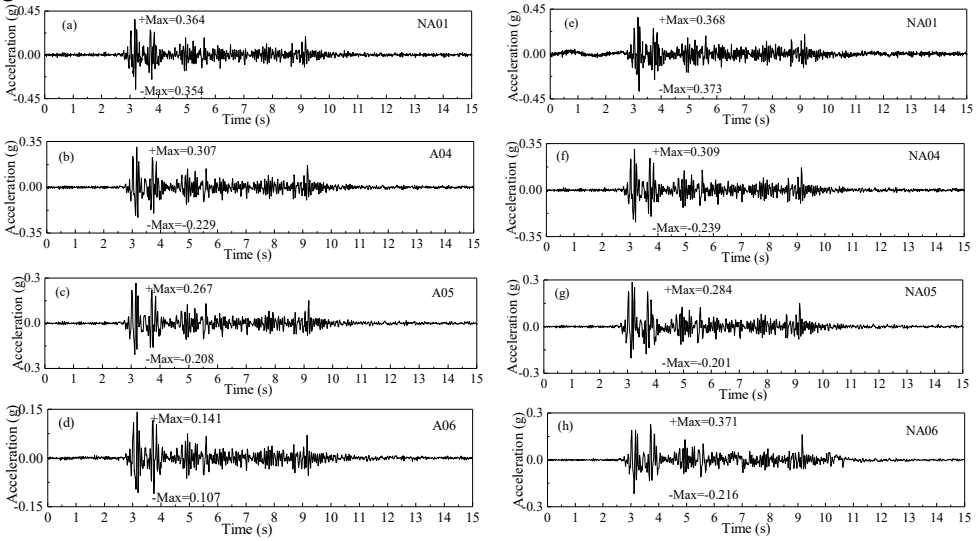

Figure 5. Acceleration histories

The acceleration response increases along the height of landslides, no matter for pile-reinforced landslide or unreinforced landslide. By comparing the acceleration response of the two landslides, it can be seen that under a realistic earthquake, the overall response of the pile-reinforced landslide is lower than that of the unreinforced landslide. However, at different parts, the acceleration response gap between the two landslides is also different. For landslide crest, the maximum acceleration is only reduced by 1.1 % after reinforced by micropiles. For middle part, the maximum acceleration is only reduced by 0.6 % after reinforced by micropiles, but for landslide toe, the maximum acceleration is reduced by 62 %. This phenomenon in the response may be associated with the presence of the micropiles that can restrain the response of surrounding soil. However, it should be pointed out that the restraining effect is limited to a very close extent, because the slope reaction at the top part of reinforced landslide becomes close to unreinforced landslides.

3.3 Residual bending moment of micropiles

Eight strain gauge couples were glued to the pile to measure the residual bending moment during shaking. Initial offsets of bending moments caused by soil self-weight were removed in order to obtain pure dynamic moments.

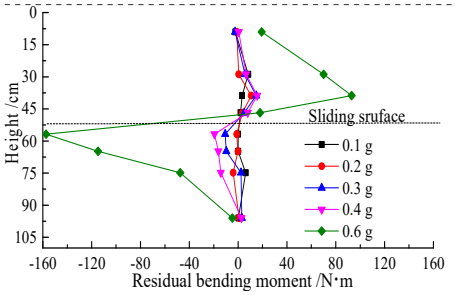

Figure 6. Residual moment of the ninth micropile under El Centro waves with different loading amplitudes

In this paper, if the front of pile is compression, the bending moment is defined as a positive value, otherwise it is defined as a negative value. The bending moments were calculated from the measured raw bending strains. Figure 6 shows the residual bending moment of the ninth micopile under El Centro waves (0.1~0.6 g).

During 0.1~0.2 g, residual bending moment of each measuring points in micropiles is tiny, which indicates that there is no obvious damage to the pile. Piles, sliding bed and sliding mass have the same movement pattern during shaking. Although the pile is subjected to repeated tensile and compressive deformation, it can recover soon after excitation. With the increase of input acceleration peak (0.3-0.6 g), landslide gradually enters the limit equilibrium state and destabilization state, and the internal damage of the pile continues to increase. Residual bending moment of micropile shows an inverse "S"-type, and positive value distributes above the slip surface, negative value below the slip surface.

It should be pointed that the maximum residual bending moment of micropile mainly distribute in 3.7 times pile diameter above the sliding surface and 1.4 times pile diameter below the sliding surface. Therefore, in seismic design of micropiles in landslides, it is necessary to strengthen these area.

4. Conclusion

Two large-scale landslide model tests were conducted by shaking table in this research to study landslide behavior and stress mechanism of micropiles under earthquake. The outcomes can be summarized as follows:

(1) Based on the test phenomenon of reinforced landslide and unreinforced landslide, it can be seen that micropiles have a good seismic performance for landslide, and the stability of the landslide can be improved by using micropiles. After reinforced with micropiles, sliding time can be delayed, sliding speed can be slowed down, and the sliding distance can be shortened.

(2) Micropiles can suppress seismic waves that in landslide. Under the same seismic wave, the acceleration response of reinforced landslide is smaller than that of unreinforced, especially in the toe of landslide.

(3) The residual bending moment of micropiles shows reverse "S"-type. The maximum residual bending moment of micropile mainly distribute in 3.7 times pile diameter above the sliding surface and 1.4 times pile diameter below the sliding surface. In seismic design of micropiles in landslides, it is necessary to strengthen these area.

Acknowledgments

This study is financially supported by the National Nature Science Fund Projects (Grants No. 41572261 and 41502277) and the Fundamental Research Funds for the Central Universities (Grant No. 310826175029)

References

[1] Huang R Q and Zhao J J 2013. Analysis of an anti-dip landslide triggered by the 2008 Wenchuan earthquake in China. Nat Hazards. 68:1021-1039.
[2] Wasowski J, Keefer D K and Lee C T 2011. Toward the next generation of research on earthquake-induced landslides: current issues and future challenges. Eng Geol. 122:1-8.
[3] Bruce D A and Juran I 1997. Drilled and grouted micropiles:State-of-practice review [R]. US Federal Highway Administration,Washington, D C: Aluminum Company.
[4] Sun S W, Zhu B Z and Wang J C 2013. Design method for stabilization of earth slopes with micropiles[J]. Soils and Foundations. 53(4):487-497.
[5] Andrew Z and Boeckmann 2006. Load transfer in micropiles for slope stabilization from test of large-scale physical models[D]. Columbia: University of Missouri-Columbia.
[6] Cai F and Ugai, K 2000. Numerical analysis of the stability of a slope reinforced with piles. Soils and Foundations. 40 (1), 73-84.
[7] Moncarz P D and Krawinkler H 1981. Theory and application of experimental model analysis in earthquake engineering. Report No. 50. Stanford, CA: Dept. of Civil Engineering and Environmental Engineering, Stanford University.